Mineralium Deposita (2005) 39: 960–969
DOI 10.1007/s00126-004-0451-y

ARTICLE

Lianchang Zhang · Wenjiao Xiao · Kezhang Qin
Wenjun Qu · Andao Du

Re–Os isotopic dating of molybdenite and pyrite in the Baishan Mo–Re deposit, eastern Tianshan, NW China, and its geological significance

Received: 29 January 2004 / Accepted: 10 October 2004 / Published online: 11 December 2004
© Springer-Verlag 2004

Abstract The Baishan Mo–Re deposit is located in the eastern section of the eastern Tianshan orogenic belt, NW China. The deposit has a grade of 0.06% Mo and a high content of rhenium of 1.4 g/t. Rhenium and osmium isotopes in sulfide minerals from the Baishan deposit are used to determine the age of mineralization. Rhenium concentrations in molybdenite samples are between 74 and 250 μg/g. Analysis of eight molybdenite samples yields an isochron age of 224.8 ± 4.5 Ma (2σ). Pyrite samples have rhenium and osmium concentrations varying in the range 33.4–330.6 ng/g and 0.08–0.81 ng/g, respectively. Isotope data on seven pyrite samples yield an isochron age of 225 ± 12 Ma (2σ) on the $^{187}Re/^{188}Os$ versus $^{187}Os/^{188}Os$ plot and an age of 233 ± 14 Ma (2σ) on the ^{187}Os versus ^{187}Re correlation diagram. The ages of molybdenite and pyrite are consistent within the analytical errors. Combined with field observations, the data indicate that Mo–Re mineralization in the Baishan deposit is produced by a magmatic-hydrothermal event in an intracontinental extensional setting after late Paleozoic orogeny. The initial $^{187}Os/^{188}Os$ ratio of pyrite is 0.3 ± 0.07. The $\delta^{34}S$ values of molybdenite vary from +0.5 to +3.6‰. Both data indicate that mineralization is derived mainly from a mantle source.

Editorial handling: J. Richards

L. Zhang (✉) · W. Xiao · K. Qin
Key Laboratory of Mineral Resources,
Institute of Geology and Geophysics,
Chinese Academy of Sciences, P.O.BOX 9825,
Beijing, 100029, China
E-mail: lczhang@mail.igcas.ac.cn, zhanglianchang@yahoo.com.cn
Tel.: +86-10-62008126
Fax: +86-10-62010846

W. Qu · A. Du
National Research Center of Geoanalysis,
Beijing, 100037, China

Keywords Re–Os isotopic dating · Mo–Re deposit · Geodynamic evolution · Eastern Tianshan

Introduction

The eastern Tianshan region has recently emerged as an important metallogenic ore province in China. More than ten larger porphyry copper–molybdenum, orogenic gold, magmatic copper–nickel, and epithermal gold deposits have been discovered in the eastern Tianshan orogen since the late-1980s. The radiometric ages of these deposits (Table 1) were determined by several researchers (Li et al. 1998; Chen et al. 1999; Rui et al. 2002a; Mao et al. 2003; Qin et al. 2003; Zhang et al. 2003a, 2003b). Isotopic data available show that most of these deposits were formed in the late Paleozoic (e.g. Tuwu–Yandong porphyry copper deposit; Kanggur gold deposit; Huangshang copper–nickel deposit; Shiyingtan gold vein I and II, Fig. 1). Therefore, the main metallogenic epoch in the Tianshan region is considered of Variscan age (Pirajno et al. 1997; Li et al. 1998; Mao et al. 2003; Qin et al. 2003).

However, Mesozoic ages of intrusions and mineralization in the eastern Tianshan have been repeatedly reported in recent years (Chen et al. 1999; Zhang et al. 2003b). This paper, based on the geochronology of the Baishan Mo–Re deposit, gives further evidence of a Mesozoic mineralization event.

Mapping by the Xinjiang Bureau of Geology and Mineral Resources (XBGMR) shows that some Mesozoic granites (245–180 Ma, XBGMR 2001, unpublished data; Deng et al. 2003) are emplaced adjacent to the Baishan Mo–Re deposit. However, so far there is no direct information on the age of ore formation. In this study, molybdenite and pyrite samples from the Baishan deposit were chosen for Re–Os isotope measurements in order to constrain the timing of mineralization. The

Table 1 Age data on the Kanggurtag Au–Cu–Mo metallogenic belt in eastern Tianshan

Deposit	Dating samples		Dating method	Age (Ma)	Reference
Tuwu Cu–(Mo)	Host rock	Volcanic rocks	Zircon U–Pb	416–361	Rui et al. (2002b)
		Plagiogranite porphyry	Zircon U–Pb	358–367	
			Rb–Sr isochron	369 ± 69	
	Ore	Molybdenite	Re–Os isochron	322.7 ± 3	
Yandong Cu–(Mo)	Host rock	Plagiogranite porphyry	Zircon U–Pb	356 ± 8	Qin et al. (2003)
	Ore	Quartz	Ar–Ar	347.3 ± 2.1	
		Sericite	K–Ar	341.2 ± 4.9	
Kanggur Au	Host rock	Altered andesite	Rb–Sr isochron	290 ± 5	Zhang et al. (2003a)
		Ryolite porphyry	Rb–Sr isochron	300 ± 13	
		Quartz–syenite porphyry	Zircon evaporation	299 ± 18	
		Tonalite	Rb–Sr isochron	282 ± 16	
			Zircon U–Pb	275 ± 7	
	Ore	Quartz, Stage-II	Rb–Sr isochron	282.3 ± 5	
		Magnetite–pyrite, Stage-II	Sm–Nd isochron	290.4 ± 7.2	
		Quartz, stage-III	Rb–Sr isochron	258 ± 21	
		Quartz, stage-IV	Rb–Sr isochron	254 ± 7	
Huangshan Cu–Ni	Host rock	Gabbro	Zircon U–Pb	285 ± 1.2	Qin et al. (2003)
		Ultrabasic-basic complex	Sm–Nd isochron	308.9 ± 10.7	Li et al. (1998)
	Ore		Sm–Nd isochron	305.4 ± 2.4	
			Re–Os isochron	282 ± 20	Mao et al. (2003)
Shiyingtan (Xitan) Au	Host rock	Andesite	Rb–Sr isochron	285 ± 12	Zhang et al. (2003b)
		Granite porphyry	Rb–Sr isochron	266 ± 3	
		Cryptoexplosion breccia	Rb–Sr isochron	261.6 ± 7	
		Rhyolite tuff	Rb–Sr isochron	256.8 ± 13	
	Ore	Quartz, ore vein I	Rb–Sr isochron on	288 ± 7	
		Quartz, ore vein II	Rb–Sr isochr	276 ± 7	
		Quartz, ore vein III	Rb–Sr isochron	244 ± 9	
Jinwuozi Au	Ore	Quartz	Rb–Sr isochron	228–230	Chen et al. (1999)
Baishan Mo–Re	Ore	Molybdenite	Re–Os isochron	224.8 ± 4.5	This study
		Pyrite	Re–Os isochron	225 ± 12	

source of the ore-forming fluids and the tectonic setting are also discussed.

Geological setting

The east Tianshan mountains, a part of the central Asian Paleozoic collisional orogenic belt, have been studied by many researchers (Windley et al. 1990; Allen et al. 1992, 1993; He et al. 1994; Biske and Shilov 1998; Qin et al. 2003; Xiao et al. 2004). The main structures of the orogen are characterized by a series of approximately east-west-trending faults, including the regional-scale Kalamaili fault (Late Paleozoic suture), Kanggurtag fault, Kushui (or Yamansu) fault, and Weiya fault (Fig. 1). Of these faults, the Kanggurtag fault, expressed by mylonite, tectono-clastic rocks, tectonic lenses, and breccia, is an important structural zone along which intense magmatic activity and associated mineralization took place (Ma et al. 1997; Zhang et al. 2004). The Dananhu–Tousuquan Paleozoic island arc consisting mainly of Devonian to Carboniferous (locally also Ordovician-Silurian, Qin et al. 2003) volcanic-intrusive rocks and hosting most of the porphyry copper deposits (e.g. Tuwu and Yandong) occurs to the north of the Kanggurtag fault (Fig.1). The Kanggurtag–Huangshan Late Paleozoic arc-related basin, consisting of Carboniferous sedimentary rocks, some Cu–Ni deposits associated with mafic complexes (e.g. Huangshan and Huangshandong), and Cu–Mo (Re) deposits related to granite porphyry (e.g. Baishan Mo–Re), is located between the Kanggurtag and Kushui faults. The Carboniferous Aqishan-Yamansu volcanic arc, and associated Au deposits (e.g. Shiyingtan Au, Kanggur Au; Fig. 1), are located between the Kushui and Weiya faults. The middle Tianshan block consisting of Precambrian and early Paleozoic metamorphic rocks is located south of the Weiya fault.

Intrusive activity in the eastern Tianshan mainly includes Variscan (350–270 Ma) granite, plagiogranite porphyry, tonalite, quartz porphyry, dacite porphyry, and mafic-ultramafic bodies. They are related to most of the gold–copper mineralizations. However, there are also some Mesozoic granites reported recently in the eastern Tianshan, such as the Weiya granite, which has a SHRIMP zircon age of 233–246 Ma (Gu et al. 2004, unpublished data) and Ar–Ar age of 223–246 Ma (Li et al. 2002), the Xiaobaishitou granite (located 20 km northeast of Weiya) with a SHRIMP zircon age of 249 ± 3 Ma, and the Baishitou granite (40 km northeast of Weiya) with a Rb–Sr isochron age of 209 ± 9.6 Ma (Gu et al. 2003).

The development of some metal ore deposits in the eastern Tianshan is closely related to subduction and closure of the ancient Tianshan ocean intervening between the Tarim and Siberian plates (He et al. 1994; Qin et al. 2003; Zhang et al. 2004). From Late Devonian to

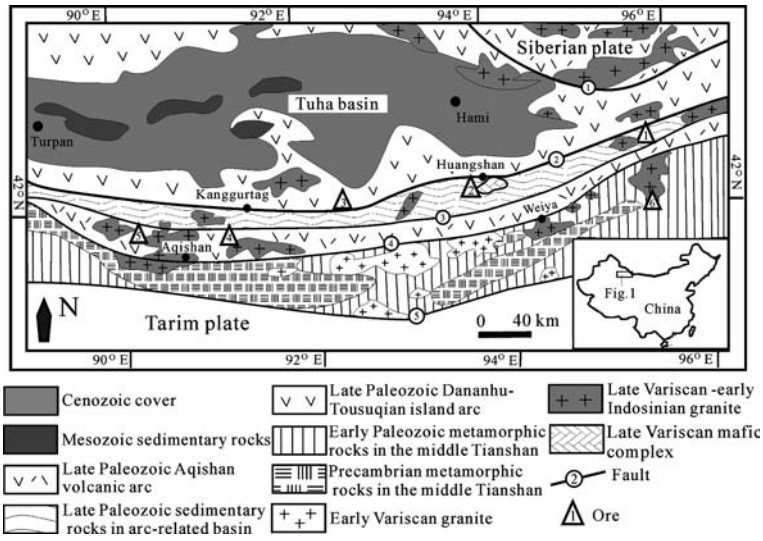

Fig. 1 Simplified geological map of the eastern Tianshan, NW China. Numbers in triangles (1–6) show location of deposits: (1) Baishan Mo–Re deposit; (2) Huangshan Cu–Ni deposit; (3) Tuwu–Yandong Cu (Mo) deposit; (4) Kanggur Au deposit; (5) Shiyingtan Au deposit; (6) Jinwozi Au deposit. The faults in Fig. 1 are: 1 Kalamaili fault; 2 Kanggurtag fault; 3 Kushui fault; 4 Weiya fault; 5 Kumishi fault

Early Carboniferous, the northern margin of the Tarim plate was a passive continental margin, whereas the ancient Tianshan ocean was subducted to the south along the Kalamaili fault, resulting in the development of the Dananhu–Tousuquan magmatic arc and associated porphyry-type Cu–Mo deposits. In Late Carboniferous, the ancient Tianshan ocean was closed and continent–continent collision occurred, leading to the formation of the east Tianshan orogen and orogenic Au deposits. The collisional event was followed by an extensional event in the Permian, large ultramafic–mafic complexes were emplaced, and a number of large-scale magmatic copper–nickel ore deposits were formed along the Kanggurtag fault. In Early Mesozoic, the tectonic evolution of the east Tianshan is characterized by post-orogenic extension with associated intrusion of granites and volcanic hydrothermal activity (i.e. Jinwozi Au, Shiyingtan III Au and Baishan Mo–Re etc.).

Local geology and sampling

The Baishan porphyry Mo–Re deposit, located ~140 km southeast (42°31′N, 95°55′E) of Hami city, is situated 2 km south of the Kanggurtag fault. The host rocks are composed of sedimentary rocks of the Lower Carboniferous Gandun Formation (Fig. 2). The sedimentary rocks are divided into four sequences (Zhou et al. 1996). The first sequence consists of siltstone interlayered with carbonaceous shale. The second sequence is composed of tuffaceous graywacke interlayered with tuff and basalt. The third sequence contains graywacke, tuff, and shale.

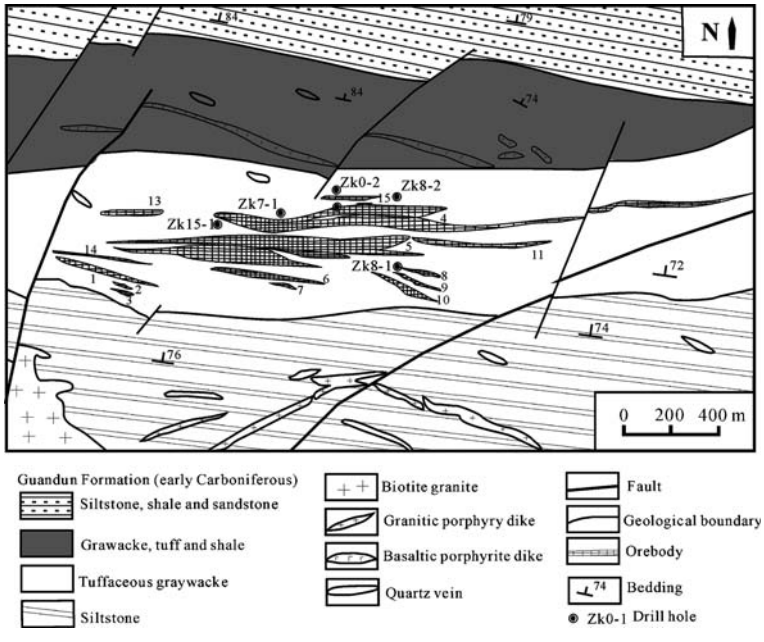

Fig. 2 Geological map of the Baishan Mo–Re deposit (modified from Deng et al. 2003)

The fourth sequence consists of siltstone, carbonaceous shale, and sandstone. The stratigraphic units trend WNW and dip ENE with an angle of 65–80°. The sedimentary rocks are thermometamorphically overprinted by deeper-seated intrusive rocks (Deng et al. 2003).

Some granitic porphyries occur as stocks and dikes in the south of the mineralized area (Fig. 2). The porphyry dikes exhibit minor pyrite and molybdenite mineralization. An unmineralized biotite granite is emplaced 1.5 km southwest of the mining area. The granite body cuts the granitic porphyry dikes, which implies the intrusion of the granite as a late event. A zircon SHRIMP U–Pb age of 181 ± 3 Ma recently obtained (Li et al. 2004, unpublished data) further indicates that the granite was intruded after Mo–Re mineralization. In the ore district (Fig. 2), minor mineralized quartz veins are widely developed. A stratabound-fracture zone is recognized, which hosts the main mineralization trending EW, and dipping north with an angle of 60–70°. A group of NE-trending faults are post-ore structures.

More than 16 mineralized bodies have been identified and 7 of these are rich orebodies (No. 4, 5, 1, 8, 9, 10 and 15; Fig. 2). Some of the larger orebodies vary between ~2 and 124 m in thickness, and 100–2,000 m in length (e.g. No. 4 and 5). They trend 85° and dip north with an angle of 65–75°. In dipping direction, the explored orebodies extend over 600 m in depth. These orebodies exhibit stratiform and lenticular shape. The average grade of the ore is 0.06% Mo (range from 0.03 to 0.14%) and 1.4 g/t Re (range from 0.7 to 1.9 g/t; Zhou et al. 1996).

In accordance with the mineral association and their occurrence, the ores can be divided into three types, i.e., molybdenite–pyrite–quartz vein, molybdenite–polymetallic sulfide–quartz vein and molybdenite-bearing altered rock. The main ore minerals include molybdenite, chalcopyrite, and pyrite, with minor pyrrhotite, magnetite, galena, sphalerite, and marcasite. The gangue minerals mainly include quartz, sericite and microcline, secondary biotite, calcite, and chlorite. The size of molybdenite ranges from 0.2 to 0.6 mm (individually up to 2 mm). Ores are characterized by subhedral-euhedral textures, veinlet-disseminated and brecciated structures.

Hydrothermal alteration is strongly developed around the orebodies, and includes phyllic and potassic alteration, biotitization, chloritization, and carbonatization. Phyllic alteration, occupying the central part of the alteration zones, consists dominantly of sericite and quartz. This zone hosts most of the molybdenite. Potassic alteration is the most conspicuous feature of the altered zones in the deposit. It is characterized by the formation of microcline throughout the orebody. Chloritization is weakly developed and related to polymetallic sulfides, whereas carbonatization is related to a late-stage vein composed of quartz and calcite. According to mineral assemblages and crosscutting relationships of the ore veins, four hydrothermal stages and one supergene stage can be identified (Table 2). The first mineralization stage (I) is characterized by quartz veins, with magnetite and ilmenite. The second stage (II) is an assemblage consisting of quartz, pyrite, and a little molybdenite. The third stage (III, main mineralization stage) consists of polymetallic sulfides including molybdenite, chalcopyrite, and pyrite, with minor galena and sphalerite. The fourth stage (IV) is marked by barren calcite-quartz veins. The supergene assemblage, only seen at the surface of the ore district, consists of copper, iron, and molybdenum oxides.

Table 2

Stage / Mineral	Hydrothermal				Supergene
	I	II	III	IV	
Molybdenite					
Pyrite					
Marcasite					
Chalcopyrite					
Galena					
Sphalerite					
Pyrrhotite					
Magnetite					
Ilmenite					
Quartz					
Calcite					
Microcline					
Biotite					
Pyrrhosiderite					
Malachite					
Gypsum					
Jarosite					
Ferrimolybdite					

According to drillcore samples (ZK15-1, 600 m in depth), an altered and mineralized granitic porphyry dike was found at a depth of ~580 m (Deng et al. 2003). We further infer that a large granite porphyry body was emplaced at the depth. Based on studies of ore geology and mineral assemblages, it is suggested that the Baishan Mo–Re deposit is of quartz vein-porphyry type.

Two groups of samples were collected from drill hole ZK15-1 in the Baishan mine area (Fig. 2). One of them (BSH-302–309), molybdenite, representing the main mineralization stage (III), was collected from 220–280 m at the depth of the central part of orebody 5. The molybdenite occurs on veinlets dissemination. The second sample (BSH-F21–F27) consists of pyrite of mineralization stage II and was collected from 30–100 m depth, at the top of orebody 5; pyrite occurs or veinlets in the orebody.

Chemical procedure and analytical technique

Re–Os isotopic analyses were performed in the National Research Center of Geoanalysis, Chinese Academy of Geosciences. The details of the chemical procedure have been described by Du et al. (1995, 2001), Shirey and Walker (1995), Stein et al. (1998), and Markey et al. (1998). They are briefly described here.

The Carius tube (a thick-walled borosilicate glass ampoule) digestion technique was used. The weighed sample was loaded in a Carius tube through a long thin-neck funnel. The mixed ^{190}Os and ^{185}Re spike solution and 2 ml of 10 N HCl and 6 ml of 16 N HNO_3 were added while the bottom part of the tube was frozen at −80 to −50°C in an ethanol-liquid nitrogen slush; the top was sealed using an oxygen–propane torch. The tube was then placed in a stainless-steel jacket and heated for 10 h at 230°C. Upon cooling, the bottom part of the tube was kept frozen, the neck of the tube was broken, and the contents of the tube were poured into a distillation flask and the residue was washed out with 40 ml of water.

Separation of osmium by distillation and separation of rhenium by extraction was performed based on the analytical method from Du et al. (1995 and 2001). A TJA PQ-EXCELL ICP-MS was used for the determination of the Re and Os isotope ratio.

Average blanks for the total Carius tube procedure were ca. 10 pg Re and ca. 1 pg Os. The analytical reliability was tested by repeated analyses of molybdenite standard HLP-5 from a carbonatite vein-type molybdenum-lead deposit in the Jinduicheng–Huanglongpu area of Shaanxi Province, China. Fifteen samples were analyzed over a period of 5 months. The uncertainty in each individual age determination was about 0.35% including the uncertainty of the decay constant of ^{187}Re, uncertainty in isotope ratio measurement, and spike calibrations. The average Re–Os age for HLP-5 is 221.3 ± 0.3 Ma (95% confidence limit, Stein et al. 1997). Median age and mean absolute deviation were 221.34 ± 0.12 Ma. The average Re concentration was 283.71 ± 1.54 μg/g. The average Os concentration was 657.95 ± 4.74 ng/g.

Results

The concentrations of Re and Os and the osmium isotopic compositions of molybdenite and pyrite from the Baishan Mo–Re deposit are shown in Tables 3 and 4. The total Re and Os concentrations of molybdenite range from 74 to 250 μg/g and 0.18 to 0.60 μg/g, respectively, whereas those of pyrite vary from 93 to 331 ng/g and 0.1 to 0.8 ng/g, respectively.

As molybdenite has extraordinarily high Re/Os ratios, the Re–Os chronometer is used for dating. Raith and Stein (2000) suggested that molybdenite does not contain any initial or common Os, and all measured Os is monoisotopic (^{187}Os), the product of decay of ^{187}Re. But, analysis actually indicates that molybdenite from some deposits contains minor common Os or initial Os (Mao et al. 2002; Hou et al. 2004). Our analyses indicate

Table 3 Re–Os isotopic data for molybdenite from the Baishan Mo–Re deposit, eastern Tianshan

Sample No.	Sample weight (g)	Re (μg/g)	^{187}Re (μg/g)	^{187}Os (μg/g)	Model age (Ma)
BSH-302	0.07645	167.2 (1.6)	105.1 (1.0)	0.389 (0.003)	222.0 (3.5)
BSH-303	0.05872	194.5 (1.7)	122.3 (1.1)	0.467 (0.003)	229.0 (3.5)
BSH-304	0.04475	188.0 (1.8)	118.2 (1.2)	0.451 (0.004)	228.6 (3.7)
BSH-305	0.05149	73.5 (0.7)	46.2 (0.4)	0.177 (0.001)	229.4 (3.6)
BSH-306	0.00671	238.2 (2.6)	149.7 (1.6)	0.570 (0.004)	227.9 (3.8)
BSH-307	0.00626	249.7 (2.8)	157.0 (1.7)	0.598 (0.004)	228.1 (3.9)
BSH-308	0.00299	107.1 (1.1)	67.3 (0.7)	0.258 (0.001)	229.9 (3.7)
BSH-309	0.00714	236.7 (2.5)	148.8 (1.6)	0.552 (0.004)	222.3 (3.6)

Enriched ^{190}Os and ^{185}Re were obtained from the Oak Ridge National Laboratory. Decay constant: $\lambda(^{187}\text{Re}) = 1.666\times10^{-11}$/year (Smoliar et al. 1996). The uncertainty in each individual age determination was about 0.35% including the uncertainty of the decay constant of ^{187}Re, uncertainty in isotope ratio measurement, and spike calibration. The concentrations of common Os in molybdenite were determined as lower than 0.05 ng/g and can be ignored

Model ages for the deposit were calculated by assuming that the initial abundance of ^{187}Os is zero. Isochron ages for all samples from the Baishan deposit were calculated by using *Isoplot* Model 3 with 2% input error. The numbers within the brackets in the table are measurement errors, and correspond to the last digit of analytical data in front of the brackets

Table 4 Re–Os isotopic data for pyrite from the Baishan Mo–Re deposit, eastern Tianshan

Sample No.	Sample Weight (g)	Total Re (ng/g)		^{187}Re (ng/g)		Common Os (ng/g)		Total Os (ng/g)		^{187}Os (ng/g)		^{187}Re/^{188}Os		^{187}Os/^{188}Os	
		Re	2σ	^{187}Re	2σ	Os	2σ	Os	2σ	^{187}Os	2σ	Ratio	2σ	Ratio	2σ
BSH-F21	0.20034	42.2	0.4	26.5	0.3	0.0207	0.001	0.124	0.001	0.104	0.001	9,751	98	38.3	0.3
BSH-F22	0.20928	63.1	0.7	39.7	0.4	0.0259	0.001	0.173	0.001	0.148	0.001	11,678	131	43.5	0.3
BSH-F23	0.20327	33.4	0.3	21.0	0.2	0.0152	0.001	0.083	0.001	0.068	0.001	10,513	94	34.3	0.3
BSH-F24	0.20123	228.4	2.5	143.5	1.6	0.0093	0.004	0.550	0.004	0.541	0.004	116,937	1300	440.4	3.3
BSH-F25	0.11525	330.6	4.4	207.8	2.8	0.0058	0.006	0.810	0.006	0.804	0.006	272,442	3638	1054.0	7.6
BSH-F26	0.20012	92.7	1.1	58.3	0.7	0.0061	0.001	0.212	0.001	0.206	0.001	72,613	849	256.1	1.7
BSH-F27	0.20562	166.7	1.9	104.8	1.2	0.1137	0.004	0.525	0.005	0.413	0.004	7,010	82	27.6	0.3

Enriched ^{190}Os and ^{185}Re were obtained from the Oak Ridge National Laboratory. Decay constant: $\lambda(^{187}\text{Re}) = 1.666\times10^{-11}$/year (Smoliar et al. 1996). The uncertainty in each individual age determination was about 0.35% including the uncertainty of the decay constant of ^{187}Re, uncertainty in isotope ratio measurement, and spike calibrations

that the concentrations of common Os in molybdenite from the Baishan deposit is <0.05 ng/g. In contrast to the ^{187}Os value of ~170 to 600 ng/g (Table 3), the common Os values can be ignored (close to zero). Therefore, the Re–Os dating of molybdenite is based on a simplified age equation, that is, $^{187}\text{Os} = {}^{187}\text{Re}\,(e^{\lambda t}-1)$.

A regression analysis was applied to eight analytical data of molybdenite, which yields an isochron with an age of 224.8 ± 4.5 Ma (2σ), initial ^{187}Os of 0.0038 ± 0.0066, and mean square weighted deviation (MSWD) of 1.2 (Fig. 3). Model ages for individual analyses range from 222.0 ± 3.5 to 229.9 ± 3.7 Ma (Table 3).

Stein et al. (2000) suggested that low-level, highly radiogenic sulfide minerals, recognized by ^{187}Re/^{188}Os ratios of ≥5,000, must be plotted in ^{187}Re–^{187}Os space to obtain meaningful precise ages. Barra et al. (2003) found that reliable geochronological and tracer information can be obtained using the ^{187}Re/^{188}Os versus ^{187}Os/^{188}Os isochron plot. For the Baishan deposit, ^{187}Re/^{188}Os ratios of pyrite are greater than 5,000 (Table 4). Analyses of seven pyrites yield one isochronal age of 225 ± 12 Ma (2σ) with an initial ^{187}Os/^{188}Os of 0.3 ± 0.07 on ^{187}Re/^{188}Os versus ^{187}Os/^{188}Os plot (MSWD = 6.3, Fig. 4a), whereas another isochronal age is 233 ± 14 Ma (2σ) with an initial ^{187}Os of −0.008 on the ^{187}Os versus ^{187}Re correlation diagram (MSWD = 3.9, Fig. 4b). Consequently, the two ages of pyrite are close to error. These isochrones are calculated based on the ^{187}Re decay constant of 1.666×10^{-11}/year (Smoliar et al. 1996) and *Isoplot* software (Ludwig 1999).

Discussions

Content of rhenium and its significance

The ore from Baishan has a high concentration of Re between 0.7 and 1.9 ppm, which reflects unusually high Re concentrations in molybdenite (74 to 250 ppm, this study; 800–900 ppm, Zhou et al. 1996), higher than in most other deposits in China and infrequent in the world (Table 5). Geological exploration in recent years indicates that the deposit may reach the scale of a large Re (Mo) deposit (Nie et al. 2001; Deng et al. 2003).

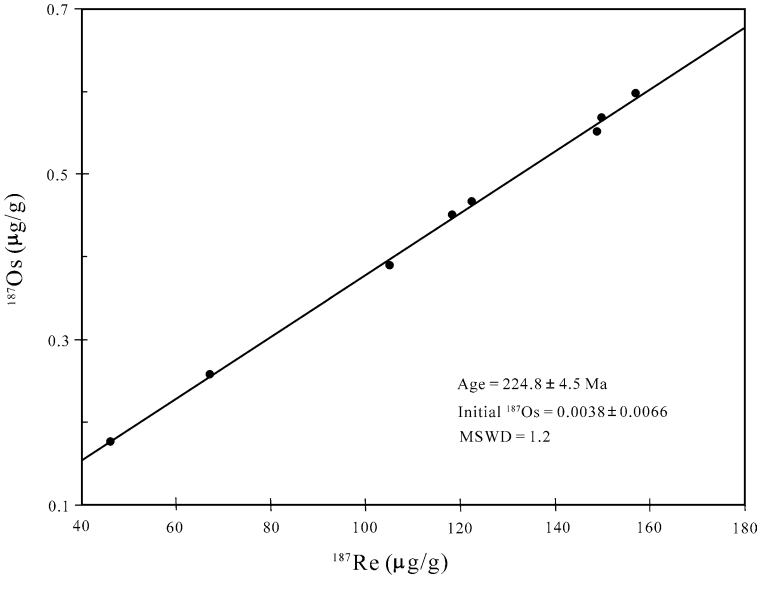

Fig. 3 Re–Os isochron plot for molybdenite samples from the Baishan Mo–Re deposit, eastern Tianshan

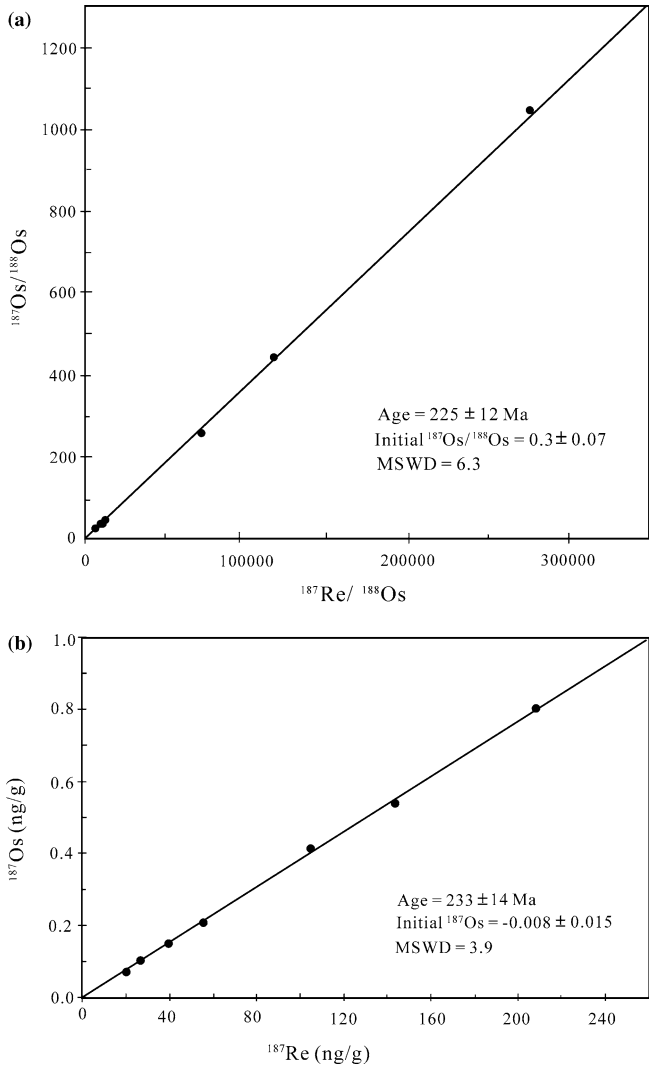

Fig. 4 (**a**) $^{187}Re/^{188}Os$ versus $^{187}Os/^{188}Os$ isochron plot for pyrite samples from the Baishan Mo–Re deposit, eastern Tianshan. (**b**) ^{187}Os versus ^{187}Re correlation diagram for pyrite samples from the Baishan Mo–Re deposit, eastern Tianshan

By gathering information on Re content in molybdenite for molybdenite-bearing deposits published in recent years, we feel that the Re contents vary greatly (Table 5). Mao et al. (1999) suggested that the Re content of molybdenite could reflect the source of the deposits. Re content would decrease from mantle-related deposits, to I-type and S-type granite-related deposits. Stein et al. (2001) also suggested that deposits with a mantle component in their source have significantly higher Re contents than those deposits that are crustally derived. We suggest that the controlling factors for Re content in molybdenite include the mineral assemblage, temperature, and source of the ore-forming material. In general, high-temperature mineral assemblages (i.e. quartz-molybdenite-chalcopyrite) have high Re content (e.g. Baishan, Gangdese, and Bagdad deposits etc.; Table 5).

Initial $^{187}Os/^{188}Os$ and source of ore-forming metals

The Re–Os isotope system has been recognized as a possible geochemical tool not only for directly dating mineralization but also for tracing the source of metals (Ruiz and Mathur1999). The $^{187}Os/^{188}Os$ ratios in the crust (0.2–10), compared to mantle values (0.11–0.15, Meisel et al. 2001), can be used to readily discern different sources (Barra et al. 2003).

The initial $^{187}Os/^{188}Os$ ratio from the pyrite isochron is 0.3 ± 0.07 (Fig. 4a), and is slightly more radiogenic than the chondritic $^{187}Os/^{188}Os$ mean ratio of 0.13 at 225 Ma. This indicates that crustal components were only a little involved in the source of osmium for pyrite. Osmium and molybdenum should have similar geochemical behavior in this system, as they are both chalcophile elements. If osmium behaves like molybdenum, then we can infer the source of Mo from understanding the source of osmium (Barra et al. 2003). According to Nie et al. (2003), there is a narrow range of positive $\delta^{34}S$ values ($+0.5$ to $+3.6‰$) for five molybdenite samples from the Baishan deposit. The $\delta^{18}O$ values of the ore fluids vary from $+4.3$ to $+5.4‰$ and the δD values from -78.8 to $-56.6‰$ (Zhou et al. 1996). These data further support the above hypothesis that the ore-forming fluids were derived mainly from a mantle source and crustal components were less involved in the ore-forming processes.

Age of mineralization and its geological significance

The Re–Os geochronometer, applied to molybdenite, has been demonstrated to be remarkably robust, even in situations of overprint by where metamorphism and deformation (Stein et al. 1998). If molybdenite does not contain any initial or common Os, all measured Os is monoisotopic (^{187}Os) as the product of decay of ^{187}Re, and the isochron age then represents the depositional age of molybdenite (Suzuki et al. 1996; Brenan et al. 2000; Barra et al., 2003). For the Baishan Mo–Re ore deposit, the analysis of eight molybdenite samples yields an isochron age of 224.8 ± 4.5 Ma (2σ) with an initial ^{187}Os of 0.0038 ± 0.0066. It is shown that the initial ^{187}Os values from the molybdenite samples are close to zero and the Re–Os isochron ages reflect the time of sulfide deposition. The Mo–Re mineralization of the Baishan deposit took place after regional low-grade metamorphism and folding, and was not influenced by later geological events.

Analyses of seven pyrite samples yield one isochron age of 225 ± 12 Ma (2σ) on the $^{187}Re/^{188}Os$ versus $^{187}Os/^{188}Os$ plot and another isochronal age of 233 ± 14 Ma (2σ) on the ^{187}Os versus ^{187}Re correlation diagram. As the pyrite samples contain minor initial Os, the molybdenite age is more reliable. However, both ages of molybdenite and pyrite are consistent within their errors, which implies that the time of ore formation for the Baishan deposit is between 225 and 233 Ma, and

Table 5 Concentrations of rhenium in molybdenite from some molybdenite-bearing deposits

Deposit	Type of deposit	Metals	Re (μg/g)	Re–Os model age (Ma)	Reference
Baishan Mo–Re deposit, Xinjiang of China	Porphyry-Vein	Mo–Re–Cu	74–250, 800–900	224.8 ± 4.5	This study, Zhou et al. (1996)
Huanglongpu Mo deposit, Shaanxi of China	Carbonatite	Mo–Pb	256–633	220–231	Huang et al. (1994)
Jinduncheng Mo deposit, Shaanxi of China	Porphyry	Mo	13–20	129–139	Huang et al. (1994)
Nannihu Mo deposit, Henan of China	Porphyry-skarn	Mo–W	22–131	146–156	Huang et al. (1994)
Chengmenshan Cu deposit, Jiangxi of China	Porphyry-skarn	Cu–Mo	10 –15	139–144	Wu et al. (1997)
Yangjiazhangzi Mo deposit, Liaoning of China	Skarn-porphyry	Mo	31–61		Wu et al. (1997)
Xiaoshigou Cu deposit, Hebei of China	Porphyry-skarn	Cu–Mo	37	134 ± 3	Huang et al. (1996)
Gangdese Cu deposit, Tibetan of China	Porphyry	Cu–Mo	87–467	13.5–14.9	Hou et al. (2004)
Shizhuyuan deposit, Hunan of China		W–Sn–Mo–Bi	1.0–1.3	130–158	Li et al. (1996)
Shameika Mo deposit, Russia	Porphyry	Mo	6.0–36.9	272–285	Mao et al. (2002)
Climax Mo deposit, USA	Porphyry	Mo	11		Huang et al. (1994)
Henderson Mo deposit, USA	Porphyry	Mo	7		Huang et al. (1994)
Bagdad Cu–Mo deposit, USA	Porphyry	Cu–Mo	330–640	72–77	Barra et al. (2003)
Western Namaqualan W (Mo) deposit, S. Africa		W–Mo	7.2–51.9	954–1018	Raith and Stein (2000)
Alpeiner Scharte Mo Deposit, Austria	Vein	Mo–W	5.5–35.6	300–307	Langthaler et al. (2004)
Hokuto Mo deposit, Japan	Vein	Mo	13.0–13.5	124.0–124.2	Suzuki et al. (1996)
Kuittilai Mo–Au prospect, Finland	Vein	Mo–Au	72.5–85.0	2773–2783	Stein et al. (1998)
Kabeliai Cu–Mo prospect, Finland	Vein	Cu–Mo	2.4–3.0	1480–1490	Stein et al. (1998)

the Mo–Re mineralization is derived from magmatic-hydrothermal activity.

Mineralization in the eastern Tianshan, reported by some researchers (Li et al. 1998; Mao et al. 2003; Qin et al. 2003), is mainly of Late Paleozoic age (330 to 260 Ma). Younger mineralization ages from the Indosinian epoch (Mesozoic) have rarely been reported in the literature. However, recent studies indicate that the ages of the Jinwuozi gold deposit are 228–230 Ma (Chen et al. 1999), the Au-bearing quartz vein III of the Shiyingtan gold deposit is 244 ± 9 Ma (Zhang et al. 2003b), and the Xiaobaishitou W–Mo deposit (20 km northeast of Weiya) is 248 Ma (Li et al. 2004, unpublished data).

Similarly, some ages of 245–211 Ma of metal deposits in the western Tianshan were reported (Ye and Ye 1999; Liu et al. 2002). These ages are close to the Re–Os ages (225–233 Ma) of molybdenite and pyrite from the Baishan Mo–Re deposit in the eastern Tianshan, and indicate that the Indosinian period is also an important mineralization epoch in the Tianshan region.

Conclusions

The Baishan deposit is controlled by a strata-bound fracture zone. The Mo–Re mineralization is ascribed to the quartz vein-porphyry type. The Re–Os isochron ages from the sulfides of the main mineralization are between 225 and 233 Ma. Based on the regional tectonic evolution, it is indicated that the deposit formed in an intracontinental extensional setting in the Early Mesozoic.

The initial $^{187}Os/^{188}Os$ ratio of 0.3 ± 0.07 and $\delta^{34}S$ values of +0.5 to +3.6‰ (Nie et al. 2003) from the sulfides indicate that the ore-forming materials are derived mainly from a mantle source.

Acknowledgements This study was financed by the Ministry of Science and Technology of China (2001CB409801 and 2001CB409805), and the Chinese Academy of Sciences (KZCX3-SW-137). Deng Gang and Yang Zaifeng, XBGMR, and Wang Qingming, Geological Survey Institute of Xinjiang Autonomous Region, offered help during sampling in the field. We are grateful for advice from Mao Jingwen. This manuscript has also benefited from constructive reviews by Robert Frei, Vickie Bennett, and Jeremy Richards.

References

Allen MB, Windley BF, Zhang C (1992) Paleozoic collisional tectonics and magmatism of the Chinese Tianshan, central Asia. Tectonophysics 220:89–115

Allen MB, Windley BF, Zhang C, Guo JH (1993) Evolution of the Turfan basin, Chinese Central Asia. Tectonics 12:889–896

Barra F, Ruiz J, Mathur R, Titley S (2003) A Re–Os study of sulfide minerals from the Bagdad porphyry Cu–Mo deposit, northern Arizona, USA. Mineralium Deposita 38:585–596

Biske YS, Shilov GG (1998) Structure of the northern margin of Tarim massif (Eastern Kokshaal area, Tien Shan). Geotectonics 32: 51–59

BrenanJM, Cherniak DJ, Rose LA (2000) Diffusion of osmium in pyrrhotite and pyrite: implications for closure of the Re–Os isotopic system. Earth Planet Sci Lett 180:399–413

Chen FW, Li HQ, Cai H (1999) The origin of the Jinwozi gold deposit in eastern Xinjiang-Evidence from isotope geochronology (in Chinese with English abstract). Geol Rev 45: 247–254

Deng G, Lu HF, Dai YC, Zhao XL (2003) A large-type quartz network-porphyry Mo deposit was discovered and proven in east Tianshan mountains (in Chinese with English abstract). Mineral Deposits 22: 317

Du A, He H, Yin N (1995) A study of the rhenium-osmium geochronometry of molybdenites. Acta Geol Sin 8:171–181

Du A, Wang S, Sun D, Zhao D, Liu D (2001) Precise Re–Os dating of molybdenite using Carius tube, NTIMS and ICPMS. In: Piestrzynski et al (eds) Mineral Deposits at the 21st Century, pp 405–407

Gu LX, Guo XQ, Zhang ZZ, Wu CZ (2003) Geochemistry and petrogenesis of a multi-zoned high Rb and F granite in eastern Tianshan (in Chinese with English abstract). Acta Petrol Sin 19:585–600

He GQ, Li MS, Liu DQ (1994) Paleozoic crustal evolution and mineralization in Xinjiang of China (in Chinese with English abstract). Xinjiang People's Publishing House, Urimqi, pp 62–245

Hou ZQ, Qu XM, Wang SX, Du A, Gao YF, Huang W (2004) Re–Os age for molybdenite from the Gangdese porphyry copper belt on Tibetan plateau: implication for geodynamic setting and duration of the Cu mineralization. Sci China D 147:221–231

Huang D, Wu C, Du A (1994) Re–Os isotopic ages and its geological significance in the eastern Qinling (in Chinese with English abstract). Mineral Deposits 13:221–230

Huang D, Du A, Wu C, Liu L, Sun Y, Zou X (1996) Metallochronology of molybdenum (-copper) deposits in the North China platform: Re–Os age of molybdenite and its geological significance (in Chinese with English abstract). Mineral Deposits 15:363–372

Langthaler KJ, Raith JG, Cornell DH, Stein HJ, Melcher F (2004) Molybdenum mineralization at Alpeiner Scharte, Tyrol (Austria): results of in-situ U–Pb zircon and Re–Os molybdenite dating (online). Mineral Petrol 82

Li S L, Li WQ, Feng XC, Dong FR (2002) Age of formation of Weiya composite stocks in eastern Tianshan mountains (in Chinese with English abstract). Xinjiang Geol 20:355–359

Li H, Mao J, Sun Y, Zhou X, He H, Du A (1996) Re–Os isotopic geochronology of the Shizhuyuan polymetallic tungsten deposit, Southern Huanan (in Chinese with English abstract). Geol Rev 42:261–267

Li HQ, Xie CF, ChangHL (1998) Study on metallogenic chronology of nonferrous and precious metallic ore deposits in northern Xinjiang, China (in Chinese with English abstract). Geological Publication House, Beijing, pp 1–263

Liu JJ, Long XR, Zheng MH (2002) The metallogenic age of Sawayaerdun gold deposit in southwastern Tianshan mountains, Xinjiang (in Chinese with English abstract). Mineral Petrol 22:19–23

Ludwig K (1999) Isoplot/Ex, version 2.0: a geochronological toolkit for Microsoft Excel. Geochronology Center, Special Publication la, Berkeley

Ma RS, Shu LS, Sun JQ (1997) Tectonic framework and crust evolution of eastern Tianshan mountains (in Chinese). Geological Publishing House, Beijing, pp 1–240

Mao JW, Zhang ZC, Zhang ZH, Du A (1999) Re–Os isotopic dating of molybdenites in the Xiaoliugou W (Mo) deposit in the northern Qinling mountains and its geological significance. Geochim Cosmochim Acta 36:1815–1818

Mao JW, Du A, Seltmann R, Yu JJ (2002) Re–Os ages for the Shameika porphyry Mo deposit and the Lipovy Log rare metal pegmatite, central Urals, Russia. Mineralium Deposita 38:251–257

Mao JW, Yang JM, Qu WJ, Du AD, Wang ZL, Han CM (2003) Re–Os age of Cu–Ni ores from the Huangshandong Cu–Ni sulfide deposit in the east Tianshan mountains and its implication for geodynamic processes. Acta Geol Sin 77:220–226

Markey R, Stein H, Morgan J (1998) Highly precise Re–Os dating for molybdenite using alkaline fusion and NTIMS. Talanta 45:935–946

Meisel T, Walker RJ, Irving AJ, Lorand JP (2001) Osmium isotopic compositions of mantle xenoliths: a global perspective. Geochim Cosmochim Acta 63:1311–1323

Nie FJ, Jiang SH, Zhao SM, Bai DM (2001) The discovery of two new precious metal deposits in the Inner Mongolia-Gansu Xinjiang juncture (Beishan) area and its geological significance. Acta Geoscientia Sin 22:397–402

Pirajno F, Luo Z, Li H, Liu S, Dong L (1997) Gold deposits in eastern Tian shan, northwestern China. Int Geol Rev 39: 891–904

Qin KZ, Zhang LC, Xiao WJ, Xu XW, Yan Z, Mao JW (2003) Overview of major Au, Cu, Ni and Fe deposits and metallogenic evolution of the eastern Tianshan mountains, northwestern China. In: Mao, Goldfarb, Seltmann, Wang, Xiao and Hart (eds) Tectonic Evolution and Metallogeny of the Chinese Altay and Tianshan. Proc Vol Interna Symp IGCP-473, IAGOD Guidebook Series 10: CERCAMS/NHM London, pp 227–248

Raith JG, Stein HJ (2000) Re–Os dating and sulfur isotopecomposition of molybdenite from tungsten deposits in western Namaqualand, South Africa: implication for ore genesis and the timing of metamorphism. Mineralium Deposita 35:41–753

Rui ZY, Wang LS, Wang YT, Liu YL (2002a) Discussion on metallogenic epoch of Tuwu and Yandong porphyry copper deposit in eastern Tianshan mountains, Xinjiang (in Chinese with English abstract). Mineral deposits 21:16–22

Rui ZY, Goldfarb RJ, Qiu YM, Zhou TH, Franco Pirajno, Yun G (2002b), Paleozoic-early Mesozoic gold deposits of the Xinjiang Autonomous Region, northwestern China: Mineralium Deposita 37:393–418

Ruiz J, Mathur R (1999) metallogenesis in continental margin: Re–Os evidence from porphyry copper deposits in Chile. In: Lambert D, Ruiz J (eds) Applications of radiogenic isotopes to ore deposit research and exploration. Rev Econ Geol 12:59–72

Shirey SB, Walker RJ (1995) Carius tube digestion for low-bank rhenium-osmium analysis. Anal Chem 67:2136–2141

Smoliar MI, Warker RJ, Morgan JW (1996) Re–Os ages of group IIA, IIIA, IVA and VIB iron meteorites. Science 271:1099–1102

Stein HJ, Markey RJ, Morgan JW, Du A, Sun Y (1997) Highly precise and accurate Re–Os ages for molybdenite from the East Qinling molybdenium belt, Shaanxi Province, China. Ecol Geol 92:827–835

Stein HJ, Sundblad K, Markey RJ, Motuza G (1998) Re–Os ages for Archean molybdenite and pyrite, Kuittila-Kivisuo, Finland, and Proterozoic molybdenite, Kabeliai, Lithuania: testing the chronometer in a metamorphic and metasomatic setting. Mineralium Deposita 33:329–345

Stein HJ, Morgan JW, Schersten A (2000) Re–Os dating of low-level highly-radiogenic (LLHR) sulfides: the Harnas gold deposit, southwest Sweden records continental scale tectonic events. Econ Geol 95:1657–1671

Stein HJ, Markey RJ, Morgan JW, Hannah JL, Schersten A (2001) The remarkable Re–Os chronometer in molybdenite: how and why it works. Terra Nova 13: 479–486

Suzuki K, Shimizu H, Masuda A (1996) Re–Os dating of molybdenites from ore deposits in Japan: Implication for the closure temperature of the Re–Os system for molybdenite and the cooling history of molybdenum ore deposit. Geochim Cosmochim Acta 60:3151–3159

Windley BF, Allen MB, Zhang C (1990) Palaeozoic accretion and Cenozoic redeformation of the Chinese Tianshan range, Central Asia. Geol 18:128–131

Wu L, Zhou X (1997) Re–Os isotopic age study of the Chengmenshan copper deposit, Jiandxi province (in Chinese with English abstract). Mineral Deposits 16:376–381

Xiao WJ, Zhang LC, Qin KZ, Sun S, Li JL (2004) Paleozoic accretionary and collisional tectonics of the eastern Chinese

Tianshan: implications for continental growth of central Asia. Am J Sci 305:1–26

Ye JH, Ye QT (1999) The metallogenic epoch and ore-bearing strata age of the Sawayaerdun gold-antimony deposit in Tianshan mountains, China. Acta Geoscientia Sin 20: 278–283

Zhang LC, Shen YC, Ji JS (2003a) Characteristics and genesis of Kanggur gold deposit in the eastern Tianshan mountains, NW China: evidence from geology, isotope distribution and chronology. Ore Geol Rev 23:71–90

Zhang LC, Ji JS, Qin KZ, Yang XK, Xie CJ, Feng CY (2003b) Geological and geochemical features of Shiyingtan Permian LS-epithermal gold deposit in east Tianshan Mts, NW China. In: Mao, Goldfarb, Seltmann, Wang, Xiao and Hart (eds) Tectonic Evolution and Metallogeny of the Chinese Altay and Tianshan. Proceedings of Vol International Symposium on IGCP-473 project. IAGOD Guidebook Series 10: CERCAMS/NHM London, pp 261–270

Zhang LC, Xiao WJ, Qin KZ, Ji JS, Yang XK (2004) Type, geological features and geodynamic significances of gold-copper deposits in the Kanggurtag metallogenic belt, eastern Tianshan, NW China. Int J Earth Sci 93:224–240

Zhou JY, Zhang B, Zhang CW, Wei GY, Lu Y, Xia J (1996) Geology of the silver, rhenium-molybdenum, gold and copper deposits in the eastern Tianshan and its adjacent regions (in Chinese). Geological Publishing House, Beijing, pp 105–133